HHS Public Access

Author manuscript

Heart Rhythm. Author manuscript; available in PMC 2016 May 01.

Published in final edited form as:

Heart Rhythm. 2015 May ; 12(5): 857–864. doi:10.1016/j.hrthm.2015.01.015.

The association of left atrial low voltage regions on electroanatomic mapping with low attenuation regions on cardiac computed tomography perfusion imaging in patients with atrial fibrillation

Zhiyu Ling, MD, PhD[*,†], **John McManigle, MD**[†], **Vadim Zipunnikov, PhD**[‡], **Farhad Pashakhanloo, BSc**[§], **Irfan M. Khurram, MD**[†], **Stefan L. Zimmerman, MD**[||], **Binu Philips, MD**[†], **Joseph E. Marine, MD, FHRS**[†], **David D. Spragg, MD, FHRS**[†], **Ashikaga Hiroshi, MD, PhD**[†], **Hugh Calkins, MD, FHRS**[†], and **Saman Nazarian, MD, PhD, FHRS**[†,#]

[*]Department of Cardiology, the Second Affiliated Hospital, Chongqing University, Chongqing, China [†]Department of Medicine/Cardiology, Johns Hopkins University, Baltimore, Maryland [‡]Department of Biostatistics, Johns Hopkins Bloomberg School of Public Health, Baltimore, Maryland [§]Biomedical Engineering, Johns Hopkins University, Baltimore, Maryland [||]Department of Radiology, Johns Hopkins University, Baltimore, Maryland [#]Department of Epidemiology, Johns Hopkins University, Baltimore, Maryland

Abstract

Background—Previous studies have shown that contrast-enhanced multidetector computed tomography (CE-MDCT) could identify ventricular fibrosis following myocardial infarction. However, whether CE-MDCT can characterize atrial low voltage regions remains unknown.

Objective—The purpose of this study is to examine the association of CE-MDCT image attenuation with left atrial low bipolar voltage regions in patients undergoing repeat ablation for recurrent atrial fibrillation (AF).

Methods—We enrolled 20 patients undergoing repeat ablation for AF recurrence. All patients underwent pre-procedural three-dimensional (3-D) CE-MDCT of the left atrium (LA) followed by voltage mapping (>100 points) of the LA during the ablation procedure. Epicardial and endocardial contours were manually drawn around LA myocardium on multi-planar CE-MDCT

Address for Correspondence: Saman Nazarian, MD, PhD; Johns Hopkins University; Carnegie 592, 600 N. Wolfe Street; Baltimore, MD 21287; Phone: 410-614-2751; Fax: 410-502-4854; snazarian@jhmi.edu.

Disclosures: Dr. Nazarian is PI for research funding to Johns Hopkins University from Biosense Webster Inc. and is also a scientific advisor to Biosense Webster Inc and Medtronic Inc. The study was supported by NIH Grants K23HL089333 and R01HL116280 to Dr. Nazarian, a China Scholarship Council grant 20115024 to Dr. Ling, as well as grants from Biosense Webster, the Dr. Francis P. Chiaramonte Foundation, and the Norbert and Louise Grunwald Research Fund. The content is solely the responsibility of the authors and does not necessarily represent the official views of the NIH.

axial images. Segmented 3-D images of the LA myocardium were reconstructed. Electroanatomic map (EAM) points were retrospectively registered to the corresponding CE-MDCT images.

Results—A total of 2028 EAM points obtained in sinus rhythm from LA endocardium were registered to the segmented LA wall CE-MDCT images. In a linear mixed model, each unit increase in local image attenuation ratio (IAR) was associated with 25.2% increase in log bipolar voltage (P=0.046) after adjusting for age, gender, body mass index, and LA volume, and clustering of data by patient and LA regions.

Conclusions—We demonstrate that IAR derived from CE-MDCT is associated with LA bipolar voltage. The potential ability to image fibrosis via CE-MDCT may provide a useful alternative in patients with contraindications to MRI.

Keywords

atrial fibrillation; cardiac computed tomography perfusion imaging; electroanatomic mapping

Introduction

Atrial fibrillation (AF) is the most common arrhythmia and is associated with increased risk of stroke, heart failure, and mortality.[1–3] Although success rates for maintenance of sinus rhythm after ablation are reasonable,[4] the procedure remains limited by recurrences.[5–7] Atrial remodeling and fibrosis have been found to associate with the recurrence of AF.[8] The location and extent of late gadolinium enhancement (LGE) on magnetic resonance imaging (MRI) has been demonstrated to benefit patient selection and assessment of ablation efficacy.[9,10] However, LGE MRI has limited spatial resolution, requires extensive expertise for proper image acquisition and analysis, is not tolerated by some patients due to claustrophobia, and is contraindicated in patients with metallic implants.[11] Recent studies have shown that contrast enhanced multidetector computed tomography (CE-MDCT) can visualize ventricular fibrosis following myocardial infarction in experimental animals and patients.[12–15] In patients with ischemic cardiomyopathy, the hypoperfusion segments on CE-MDCT matched well with abnormal voltage segments.[15] We sought to test the hypothesis that low voltage left atrial (LA) myocardium also has lower perfusion and consequently lower image attenuation on perfusion CE-MDCT.

Methods

Patient Characteristics

The study cohort includes 20 patients that underwent repeat AF ablation at our institution from November 2012 to December 2013 for recurrence after initial ablation. All 20 patients underwent pre-procedural CE-MDCT. The Johns Hopkins Institutional Review Board approved the study protocol and all subjects provided written informed consent. Follow up entailed office visits at 3 and 6 months, as well as symptom-prompted ECGs and Holter monitors.

Multislice Computed Tomography

CE-MDCT scans were performed with a commercially available 320-detector computed tomography (CT) scanner (One Aquilion, Toshiba Medical Systems, Otawara, Japan) on the same day or less than 1-week prior to the repeat AF ablation procedure. Slice collimation ranged from 320×0.5 mm, tube voltage was 80, 100 or 120 kV, depending on body habitus. Tube amperage ranged from 320 to 580mA depending on body habitus and heart rate. Image acquisition was gated to 40% of the R-R interval during a breath-hold. Beta-blockers were used at the discretion of the performing cardiologist to decrease heart rate below 80 bpm. The triphase contrast protocol includes a total volume of 60mL (70mL if body mass index >30) of the noniodinated contrast material iopamidol (Isovue 370; Bracco Diagnostics, Princeton, NJ) administered at a rate of 5–6mL/sec in the following sequence: 20mL saline test injection, 50mL (100% contrast), 20mL (50% saline, 50% contrast), and followed by 30mL saline flush. The images acquired during the first pass were used for later segmentation and analysis.

Electroanatomic Mapping

The repeat ablation was performed at 21.6 ±15.9 months after the initial ablation. All procedures were performed using a 3-dimensional electroanatomic mapping system (CARTO 3, Biosense Webster Inc, Diamond Bar, California). Detailed endocardium voltage maps of the LA were obtained with a 3.5-mm-tip with 2 mm inter-electrode spacing, irrigated ablation catheter (Thermo-Cool, Biosense Webster, Diamond Bar, CA) during sinus rhythm. To optimize ablation success,[16] patients with persistent AF were referred for external cardioversion 3–4 weeks before CE-MDCT and AF ablation. Electrograms were filtered at 30 to 400 Hz (bipolar) and 1 to 240 Hz (unipolar). Myocardial regions were considered abnormal if bipolar voltage was <0.5mV and dense fibrosis if <0.1 mV.[17–21] The CE-MDCT-derived images were registered to the electroanatomic map (EAM) using standard landmark image registration techniques (Figure 1A). The mean distance between each EAM point and the closest CE-MDCT-derived chamber wall was calculated to evaluate registration accuracy. After completion of electroanatomic mapping, a 20-electrode Lasso catheter was introduced into the LA. PV potentials were evaluated with the Lasso catheter, and reconnection sites were re-isolated using a wide circumferential approach. After ablation, patients were observed for 24 hours before discharge and were followed regularly at our outpatient clinic.

LA Wall Segmentation and Graphical Representations

The CE-MDCT images were processed off-line using Seg3D software (Version 2.1.4, University of Utah, Salt Lake City, USA). Left atrial epicardial and endocardial borders were manually contoured on multi-planar axial images (Figure 1B). Care was taken in 2-dimensional tracings of the endocardial and epicardial walls to confine the region of interest to only the LA wall and to avoid the blood pool and epicardial fat regions. The local mean LA wall attenuation measured in Hounsfield units (Hu) was obtained by using custom software written in MATLAB (The Mathworks Inc, MA, USA). The analysis software measures the geometric mean attenuation of 5-mm regions of LA myocardium. For graphical representations (not statistical comparisons), the Otsu Threshold tool was used.

The Otsu Threshold tool produces an image intensity histogram to allow the selection of histogram based threshold levels. The threshold to display colors on the attenuation maps of Figure 2 (lower panels) were manually adjusted to highlight the lowest attenuation regions in red and the highest attenuation regions in purple, similar to the voltage maps (upper panels). The color bar at the right of each lower panel specifies the original CT data attenuation (Hu).

Image and Electrogram Registration

Intra-atrial EAM points were registered to the 3D CE-MDCT images using a semi-automated, three-step process. First, the pulmonary veins were identified manually on the EAM and the image, and a similarity transform was applied to the EAM coordinates to minimize mean squared distance between the corresponding landmarks. Second, an iterative refinement to the similarity transform was used to minimize the mean squared distance between the EAM points and the boundary of the manually segmented left atrium. Finally, a non-rigid transform to further reduce the mean squared distance was determined iteratively and applied to the EAM coordinates (Figure 1C). After registration, the CE-MDCT attenuation of each EAM point was determined by taking the geometric mean of each CE-MDCT image voxel which was within 5mm of the registered EAM point coordinates and within the manual segmentation of the LA myocardium.

The image attenuation ratio (IAR), similar to image intensity ratio used for LGE MRI,[22] defined as the local LA myocardial CE-MDCT attenuation divided by the mean LA blood pool attenuation during the first pass perfusion, was calculated. To account for the regional heterogeneity of CE-MDCT image attenuation in different regions of LA, we divided the pulmonary veins (PVs) and LA posterior wall into 13 segments: the 4 PVs; the antrum of each PV; the upper posterior, middle posterior, lower posterior, mitral isthmus, and septal surfaces of the LA wall, as shown in Figure 1D.

Statistical Analyses

Continuous variables are expressed as mean ± standard deviation and categorical data as numbers or percentages. Due to the skewed nature of bipolar voltage measures, log-transformation was utilized to make the distribution more symmetric and accommodate modeling within a linear normal framework. To account for intra-patient clustering of data and patient level differences in data clusters, a linear mixed model, clustered by patient, and adjusted by age, gender, body mass index, and LA volume as level-1 variables and LA regions as the level-2 variable, was used to examine the association of LA IAR on CE-MDCT with log-bipolar atrial electrogram amplitude measures. The intra-class correlation coefficients for inter- and intra-observer variability in measuring the IAR were calculated using two-way random effects models. To estimate uncertainty associated with the sample size, we utilized a nonparametric bootstrap study to confirm the significance of the associations.[23] Statistical analyses were performed using STATA software (version 12, Stata Corp, College Station, TX).

Results

Patient Characteristics

Twenty patients (age 60.8±9.6; 10 males) with pre-procedural CE-MDCT image were enrolled in the study. Prior to the repeat procedure, 12 patients had recurrent episodes of paroxysmal AF and 8 had recurrent persistent AF. The clinical and procedural characteristics of the 20 patients are summarized in Table 1. An average number of 114.4±23.8 EAM points were sampled per patient during sinus rhythm. All patients tolerated CE-MDCT and repeat PV isolation procedures without complications.

Registration of CE-MDCT 3D Images and Electroanatomic Mapping

A total of 2140 slices in CE-MDCT axial planes from 20 patients were analyzed. A total of 2287 EAM points were registered to the CE-MDCT 3D images. Of these, 259 points were excluded from the study due to registration distance >5 mm from LA myocardium or suboptimal catheter contact evident from instability in the beat-to-beat electrogram signal. Consequently, 2028 EAM points obtained from LA endocardium were evaluated and registered to the segmented LA wall CE-MDCT 3D images. The CE-MDCT image attenuation corresponding to each EAM point, measured in Hu was obtained. After registration, the mean distance of EAM points from LA myocardium was 0.82 ±1.56 mm.

Association of LA IAR with Local Bipolar Electrograms

The average bipolar voltage was 0.65±0.51 mV (0.46 between and 0.67 within patient standard deviation). The average LA image attenuation was 140.09±45.79 Hu, and the average IAR was 0.34±0.12. In a linear mixed model, accounting for clustering of data by patients and adjusting for age, sex, body mass index and LA volume, the local LA wall CE-MDCT IAR had a positive association with log local bipolar LA voltage (P=0.046). Table 2 summarizes the linear mixed model results for the association of each variable with log-bipolar voltage.

We further examined this finding by a nonparametric bootstrap method.[23] This analysis is a type of resampling method that is useful in situations with small sample size or when the theoretical distribution of the statistic is complicated. Using this method, we created new samples of 19 patients. We then executed the multivariable analysis including those variables from the multivariable model in Table 2, and repeated the process for a total 1000 times. These new samples were taken from the original data set using sampling with replacement, so it is not identical to the original sample. This method confirmed the association between IAR and log bipolar voltage with a coefficient of 0.252 (95% CI: 0.026–0.478, P=0.029) after adjusting for age, gender, BMI, LA volume, as well as clustering by patient and adjustment for LA regions (as a level 2 variable).

On qualitative graphical representations, the electroanatomic maps (EAMs) overall correlated well with the CT generated maps. Specifically, about 80% of the maps exhibited good or intermediate qualitative similarity and 20% exhibited qualitative differences. Three sets of CE-MDCT derived image attenuation maps and corresponding EAMs from 3 patients in the study are illustrated in Figure 2. Panel A is an example of good qualitative agreement

between low voltage (<0.1mV) regions on EAM and the image attenuation map from CT. Panel B is an example of intermediate qualitative agreement between low voltage regions on EAM and the image attenuation map from CT, whereas the images in Panel C exhibit qualitative differences.

Inter- and Intra-observer Variability

A total of 535 CE-MDCT axial planes from 5 patients underwent repeat review by an independent observer. The intra-class correlation coefficient for inter-reader variability of the IAR measures was 0.905 for reliability of observations (95% CI: 0.903–0.908). The primary observer also repeated the manual contouring in 5 patients for intra-observer variability analysis. The intra-class correlation coefficient for intra-reader variability of the IAR measures was 0.940 for reliability of observations (95% CI: 0.938–0.943). The intra- and inter-observer variability data are shown in figures 3A and 3B, respectively.

Discussion

Main Findings

To the best of our knowledge, this is the first study comparing local LA endocardial bipolar voltage measures with local atrial myocardial image attenuation on CE-MDCT in patients with AF. The main finding of this study is that in patients with AF, after adjusting for confounders, the local LA IAR is independently associated with local atrial bipolar voltage.

LA Wall CE-MDCT IAR and Bipolar Voltage

Studies have shown histological changes in the left atrial myocardium of patients with AF including inflammatory infiltrates, myocyte hypertrophy, and interstitial fibrosis.[24–26] The increased interstitial fibrosis accompanied with reduced microvasculature in the fibrotic atrial myocardium results in decreased myocardial perfusion. Thus, the abnormalities of the fibrotic atrial myocardium maybe noninvasively detected by contrast enhanced CE-MDCT images. Recently, Dewland et al[27] compared the LA wall thickness and density measured from contrast enhanced CE-MDCT between 98 patients with AF and 89 controls. They found that AF was associated with reduced density in the LA anterior wall and increased density below the right inferior pulmonary vein (RIPV) and in the LA appendage. Their study suggested that CE-MDCT might be used to noninvasively assess LA myocardial abnormalities by measurement of myocardial radiographic image attenuation on perfusion images. In this study, we performed CE-MDCT in 20 patients before repeat AF ablation procedures. The extent of LA fibrosis, native or created by the first radiofrequency ablation, was quantified by high-density voltage mapping during the repeat procedure. We found that the local IAR near each EAM point is positively associated with the local bipolar voltage.

LGE MRI has been recognized as a validated imaging technique for the assessment of myocardial fibrosis.[28–31] LGE MRI offers several advantages including improved signal to noise ratio for assessment of myocardial fibrosis without radiation exposure. However, LGE MRI has limitations, including limited spatial resolution, propensity to motion artifacts, and imaging contraindications and/or artifacts in the presence of cardiac implantable devices. Additionally, LGE MRI acquisition and analysis requires extensive experience and suffers

from poor generalizability to routine clinical practice,[32, 33] due to poor image quality in patients with arrhythmia, with inability to breath hold, and with pacemakers and implantable cardioverter defibrillators.[33] In contrast, cardiac CE-MDCT is fast, widely available, easy to perform, and offers reliable image quality. In addition, CE-MDCT can provide accurate images of the coronary arteries with quantitative assessment of coronary calcification and epicardial adipose tissue.[34, 35] On the other hand, CE-MDCT exposes the patient to radiation in addition to that received from fluoroscopy. Additionally, while improving the spatial resolution, CE-MDCT has lower soft tissue resolution and contrast to noise ratio than LGE-MRI. With advancing technologies and techniques, the radiation exposure for CE-MDCT is continually decreasing and the contrast to noise ratio is improving. As a pre-procedural tool CE-MDCT can provide valuable information regarding atrial tissue characterization, in addition to 3D anatomical images with greater spatial resolution than those obtainable with MRI. Prior studies have demonstrated excellent association between myocardial infarct size on cardiac CE-MDCT, LGE-MRI, and histopathology in animal models.[12, 36, 37] Theoretically, first-pass CT or MRI imaging performed immediately after contrast material administration will also show relative hypo-enhancement of infarcted or fibrotic myocardium caused by reduced microvascular perfusion of the affected tissue. Nieman and colleagues confirmed this hypothesis in 21 patients with acute reperfused myocardial infarction; where early hypo-attenuation was differentiated from normal myocardium by both first-pass CT and MRI.[36] We do not have direct histology evidence that CE-MDCT can identify LA fibrosis; however, this feasibility study shows that the LA IAR is associated with bipolar voltage as a surrogate of fibrosis.

Limitations

This study had several limitations. First, the study sample size was small, which led to an inability to account for some patient level covariates. The small patient sample size is partially offset by the detailed high quality CE-MDCT image analysis and accurate image registration with EAM, providing >2000 registered image-electrogram points for quantitative analyses. However, future studies with a larger number of AF patients undergoing CE-MDCT prior to ablation may refine these results. Second, although care was taken to be as accurate as possible with segmentation; due to inherently thin walls of the left atrium, it is likely that segmentation may have included pixels with volume averaging of peri-atrial fat and endo-luminal contrast. This volume averaging is unavoidable, however, is expected to be uniform across the entire atrium and would equally impact IAR from both fibrotic and non-fibrotic atrial walls. Third, the anterior LA wall and the LA appendage electrograms were not densely sampled, and the association between CE-MDCT IAR and local voltage in these regions may differ from that in other LA sites. Our patients had all undergone prior catheter ablation of AF and so likely had a mixture of native and ablation-induced fibrosis. The ability of CE-MDCT to identify only native LA fibrosis needs to be validated in other patient cohorts. Finally, the study did not contain an external validation set, however, we implemented a resampling simulation study that confirmed the significance of the association.

Conclusions

We demonstrate that the local atrial IAR derived from CE-MDCT significantly associates with local atrial bipolar voltage. Although the signal to noise ratio of imaging obtained by CE-MDCT does not equal that of LGE MRI, the improved spatial resolution, and the ease of image acquisition and analysis impart significant advantages for CE-MDCT as a useful imaging alternative for tissue characterization in AF patients.

Abbreviations

AF	atrial fibrillation
LGE	late gadolinium enhancement
MRI	magnetic resonance imaging
CE-MDCT	contrast enhanced multidetector computed tomography
LA	left atrium
EAM	electroanatomic mapping
Hu	Hounsfield unit
IAR	image attenuation ratio
RIPV	right inferior pulmonary vein

References

1. Wolf PA, Abbott RD, Kannel WB. Atrial-fibrillation as an independent risk factor for stroke - the framingham-study. Stroke. 1991; 22:983–988. [PubMed: 1866765]
2. Anter E, Jessup M, Callans DJ. Atrial fibrillation and heart failure treatment considerations for a dual epidemic. Circulation. 2009; 119:2516–2525. [PubMed: 19433768]
3. Benjamin EJ, Wolf PA, D'Agostino RB, Silbershatz H, Kannel WB, Levy D. Impact of atrial fibrillation on the risk of death: The framingham heart study. Circulation. 1998; 98:946–952. [PubMed: 9737513]
4. Wann LS, Curtis AB, January CT, et al. 2011 accf/aha/hrs focused update on the management of patients with atrial fibrillation (updating the 2006 guideline): A report of the american college of cardiology foundation/american heart association task force on practice guidelines. Heart rhythm : the official journal of the Heart Rhythm Society. 2011; 8:157–176. [PubMed: 21182985]
5. Bertaglia E, Tondo C, De Simone A, Zoppo F, Mantica M, Turco P, Iuliano A, Forleo G, La Rocca V, Stabile G. Does catheter ablation cure atrial fibrillation? Single-procedure outcome of drug-refractory atrial fibrillation ablation: A 6-year multicentre experience. Europace : European pacing, arrhythmias, and cardiac electrophysiology : journal of the working groups on cardiac pacing, arrhythmias, and cardiac cellular electrophysiology of the European Society of Cardiology. 2010; 12:181–187.
6. Weerasooriya R, Khairy P, Litalien J, et al. Catheter ablation for atrial fibrillation are results maintained at 5 years of follow-up? J Am Coll Cardiol. 2011; 57:160–166. [PubMed: 21211687]
7. Wilber DJ, Pappone C, Neuzil P, et al. Comparison of antiarrhythmic drug therapy and radiofrequency catheter ablation in patients with paroxysmal atrial fibrillation: A randomized controlled trial. JAMA : the journal of the American Medical Association. 2010; 303:333–340.
8. Velagapudi P, Turagam MK, Leal MA, Kocheril AG. Atrial fibrosis: A risk stratifier for atrial fibrillation. Expert review of cardiovascular therapy. 2013; 11:155–160. [PubMed: 23405837]

9. Malcolme-Lawes LC, Juli C, Karim R, et al. Automated analysis of atrial late gadolinium enhancement imaging that correlates with endocardial voltage and clinical outcomes: A 2-center study. Heart rhythm : the official journal of the Heart Rhythm Society. 2013; 10:1184–1191. [PubMed: 23685170]
10. McGann C, Kholmovski E, Blauer J, et al. Dark regions of no-reflow on late gadolinium enhancement magnetic resonance imaging result in scar formation after atrial fibrillation ablation. J Am Coll Cardiol. 2011; 58:177–185. [PubMed: 21718914]
11. Dewey M, Schink T, Dewey CF. Claustrophobia during magnetic resonance imaging: Cohort study in over 55,000 patients. Journal of magnetic resonance imaging : JMRI. 2007; 26:1322–1327. [PubMed: 17969166]
12. Baks T, Cademartiri F, Moelker AD, Weustink AC, van Geuns RJ, Mollet NR, Krestin GP, Duncker DJ, de Feyter PJ. Multislice computed tomography and magnetic resonance imaging for the assessment of reperfused acute myocardial infarction. J Am Coll Cardiol. 2006; 48:144–152. [PubMed: 16814660]
13. Berliner JI, Kino A, Carr JC, Bonow RO, Choudhury L. Cardiac computed tomographic imaging to evaluate myocardial scarring/fibrosis in patients with hypertrophic cardiomyopathy: A comparison with cardiac magnetic resonance imaging. The international journal of cardiovascular imaging. 2013; 29:191–197. [PubMed: 22527259]
14. Lardo AC, Cordeiro MA, Silva C, et al. Contrast-enhanced multidetector computed tomography viability imaging after myocardial infarction: Characterization of myocyte death, microvascular obstruction, and chronic scar. Circulation. 2006; 113:394–404. [PubMed: 16432071]
15. Tian J, Jeudy J, Smith MF, et al. Three-dimensional contrast-enhanced multidetector ct for anatomic, dynamic, and perfusion characterization of abnormal myocardium to guide ventricular tachycardia ablations. Circulation Arrhythmia and electrophysiology. 2010; 3:496–504. [PubMed: 20657032]
16. Rivard L, Hocini M, Rostock T, et al. Improved outcome following restoration of sinus rhythm prior to catheter ablation of persistent atrial fibrillation: A comparative multicenter study. Heart rhythm : the official journal of the Heart Rhythm Society. 2012; 9:1025–1030. [PubMed: 22342863]
17. Abrams DJ, Earley MJ, Sporton SC, Kistler PM, Gatzoulis MA, Mullen MJ, Till JA, Cullen S, Walker F, Lowe MD, Deanfield JE, Schilling RJ. Comparison of noncontact and electroanatomic mapping to identify scar and arrhythmia late after the fontan procedure. Circulation. 2007; 115:1738–1746. [PubMed: 17372177]
18. Mesas CE, Augello G, Lang CCE, Gugliotta F, Vicedomini G, Sora N, De Paola AAV, Pappone C. Electroanatomic remodeling of the left atrium in patients undergoing repeat pulmonary vein ablation: Mechanistic insights and implications for ablation. J Cardiovasc Electr. 2006; 17:1279–1285.
19. Oral H, Chugh A, Good E, et al. Radiofrequency catheter ablation of chronic atrial fibrillation guided by complex electrograms. Circulation. 2007; 115:2606–2612. [PubMed: 17502567]
20. Sanders P, Morton JB, Kistler PM, Spence SJ, Davidson NC, Hussin A, Vohra JK, Sparks PB, Kalman JM. Electrophysiological and electroanatomic characterization of the atria in sinus node disease - evidence of diffuse atrial remodeling. Circulation. 2004; 109:1514–1522. [PubMed: 15007004]
21. Stevenson IH, Kistler PM, Spence SJ, Vohra JK, Sparks PB, Morton JB, Kalman JM. Scar-related right atrial macroreentrant tachycardia in patients without prior atrial surgery: Electroanatomic characterization and ablation outcome. Heart rhythm : the official journal of the Heart Rhythm Society. 2005; 2:594–601. [PubMed: 15922265]
22. Khurram IM, Beinart R, Zipunnikov V, et al. Magnetic resonance image intensity ratio, a normalized measure to enable interpatient comparability of left atrial fibrosis. Heart rhythm : the official journal of the Heart Rhythm Society. 2014; 11:85–92. [PubMed: 24096166]
23. Efron B. 1977 rietz lecture - bootstrap methods - another look at the jackknife. Ann Stat. 1979; 7:1–26.
24. Boldt A, Wetzel U, Lauschke J, Weigl J, Gummert J, Hindricks G, Kottkamp H, Dhein S. Fibrosis in left atrial tissue of patients with atrial fibrillation with and without underlying mitral valve disease. Heart. 2004; 90:400–405. [PubMed: 15020515]

25. Chimenti C, Russo MA, Carpi A, Frustaci A. Histological substrate of human atrial fibrillation. Biomed Pharmacother. 2010; 64:177–183. [PubMed: 20006465]
26. Kottkamp H. Human atrial fibrillation substrate: Towards a specific fibrotic atrial cardiomyopathy. Eur Heart J. 2013; 34:2731–2738. [PubMed: 23761394]
27. Dewland TA, Wintermark M, Vaysman A, Smith LM, Tong E, Vittinghoff E, Marcus GM. Use of computed tomography to identify atrial fibrillation associated differences in left atrial wall thickness and density. Pace. 2013; 36:55–62. [PubMed: 23106219]
28. Higuchi K, Akkaya M, Akoum N, Marrouche NF. Cardiac mri assessment of atrial fibrosis in atrial fibrillation: Implications for diagnosis and therapy. Heart. 2014; 100:590–596. [PubMed: 23619986]
29. Longobardo L, Todaro MC, Zito C, Piccione MC, Di Bella G, Oreto L, Khandheria BK, Carerj S. Role of imaging in assessment of atrial fibrosis in patients with atrial fibrillation: State-of-the-art review. Eur Heart J-Card Img. 2014; 15:1–5.
30. Oakes RS, Badger TJ, Kholmovski EG, et al. Detection and quantification of left atrial structural remodeling with delayed-enhancement magnetic resonance imaging in patients with atrial fibrillation. Circulation. 2009; 119:1758–U1123. [PubMed: 19307477]
31. Spragg DD, Khurram I, Zimmerman SL, Yarmohammadi H, Barcelon B, Needleman M, Edwards D, Marine JE, Calkins H, Nazarian S. Initial experience with magnetic resonance imaging of atrial scar and co-registration with electroanatomic voltage mapping during atrial fibrillation: Success and limitations. Heart rhythm : the official journal of the Heart Rhythm Society. 2012; 9:2003–2009. [PubMed: 23000671]
32. Sasaki T, Hansford R, Zviman MM, Kolandaivelu A, Bluemke DA, Berger RD, Calkins H, Halperin HR, Nazarian S. Quantitative assessment of artifacts on cardiac magnetic resonance imaging of patients with pacemakers and implantable cardioverter-defibrillators. Circ-Cardiovasc Imag. 2011; 4:662–U104.
33. Spiewak M, Malek LA, Misko J, Chojnowska L, Milosz B, Klopotowski M, Petryka J, Dabrowski M, Kepka C, Ruzyllo W. Comparison of different quantification methods of late gadolinium enhancement in patients with hypertrophic cardiomyopathy. Eur J Radiol. 2010; 74:E150–E154.
34. Nakanishi R, Rajani R, Cheng VY, et al. Increase in epicardial fat volume is associated with greater coronary artery calcification progression in subjects at intermediate risk by coronary calcium score: A serial study using non-contrast cardiac ct. Atherosclerosis. 2011; 218:363–368. [PubMed: 21835407]
35. Tsao HM, Hu WC, Wu MH, et al. Quantitative analysis of quantity and distribution of epicardial adipose tissue surrounding the left atrium in patients with atrial fibrillation and effect of recurrence after ablation. Am J Cardiol. 2011; 107:1498–1503. [PubMed: 21414593]
36. Nieman K, Shapiro MD, Ferencik M, Nomura CH, Abbara S, Hoffmann U, Gold HK, Jang IK, Brady TJ, Cury RC. Reperfused myocardial infarction: Contrast-enhanced 64-section ct in comparison to mr imaging. Radiology. 2008; 247:49–56. [PubMed: 18372464]
37. Schuleri KH, Centola M, Choi SH, Evers KS, Dawoud F, George RT, Lima JA, Lardo AC. Ct for evaluation of myocardial cell therapy in heart failure: A comparison with cmr imaging. JACC. Cardiovascular imaging. 2011; 4:1284–1293. [PubMed: 22172785]

Clinical Perspective

Despite advancements in atrial fibrillation (AF) catheter ablation, reported recurrence rates after ablation remain high especially in patients with extensive LA fibrosis. Late gadolinium enhancement (LGE) magnetic resonance imaging (MRI) has been recognized as a validated imaging technique for the assessment of myocardial fibrosis. However, MRI has limitations, including limited spatial resolution, propensity to motion artifacts, and imaging contraindications and/or artifacts in the presence of cardiac implantable devices. In this study, we demonstrate an association between local LA endocardial bipolar voltage measures and atrial myocardial image attenuation ratio (IAR) on contrast-enhanced multidetector computed tomography (CE-MDCT) in patients with AF. Based upon these results, CE-MDCT may provide a useful alternative for risk stratification and/or procedural planning in patients with AF.

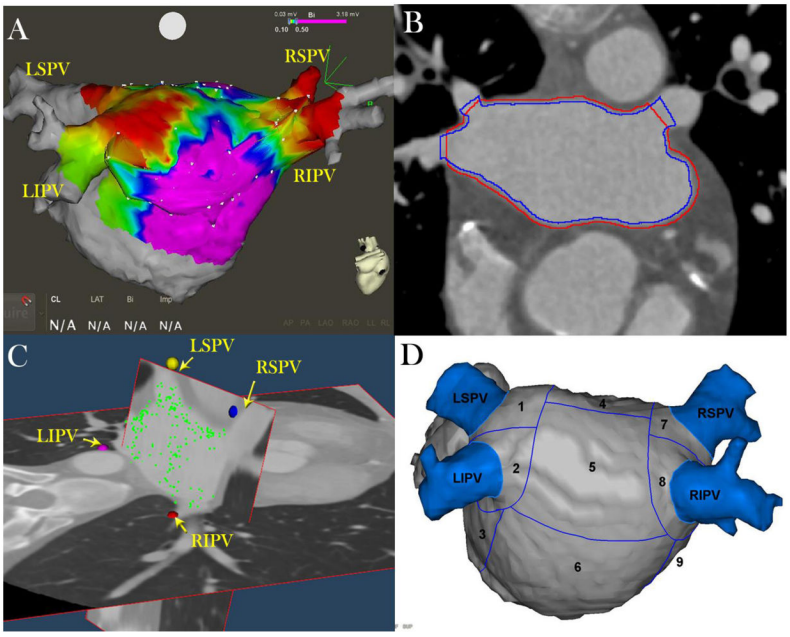

Figure 1. Image and Electrogram analysis Methodology

Panel A: EAM points (white points) obtained invasively during sinus rhythm and merged with the left atrial (LA) endocardial shell obtained from the CE-MDCT image prior to the procedure. Regions with bipolar voltage <0.1 mV are highlighted in red and healthy regions with voltage >0.5 mV are highlighted in purple.

Panel B: Manually drawn endo- (blue line) and epicardial (red line) contours on CE-MDCT axial planes. The lines are drawn to cross each other at the pulmonary vein ostia to exclude the blood pool intensities from analysis.

Panel C: EAM points (green dots) are registered to the LA wall on 3D CE-MDCT images. The posterior wall has been hidden to allow the visualization of the PV ostia and the roof; therefore, in this image the posterior wall points are not visualized next to the wall.

Panel D: Summary of 13 left atrial segments in the posterior wall and the antrum of PVs. LIPV = left interior pulmonary vein; LSPV = left superior pulmonary vein; RIPV = right inferior pulmonary vein; RSPV = right superior pulmonary vein; 1=LSPV antrum; 2=LIPV antrum; 3= mitral isthmus region; 4= upper posterior region; 5= middle posterior region; 6= lower posterior region; 7=RSPV antrum;8=RIPV antrum;9= septal region.

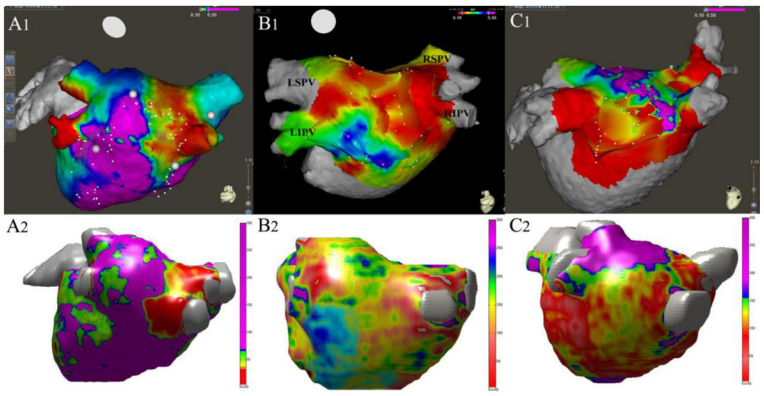

Figure 2. CE-MDCT Attenuation versus EAM Maps

In agreement with the multivariable models, the CT generated maps revealed overall qualitative agreement with the EAMs. The figure illustrates three sets of CE-MDCT attenuation and EAMs from different patients in our study. The upper panels (A1, B1, C1) illustrate the EAMs performed in repeat pulmonary vein isolation patients that highlight low voltage (<0.1mV) regions in red. The lower panels (A2, B2, C2) illustrate the CT derived LA image attenuation map in the same patients as those in the upper panels, where the low image attenuation regions within the LA are highlighted in red and the high image attenuation regions are highlighted in purple. The color bar at the right of each lower panel describes the original CT data intensity (Hu). Panel A is an example of good qualitative similarity between the EAM and CT attenuation map. Panel B shows an example of intermediate qualitative agreement, and Panel C shows an example of an outlier patient with relatively poor agreement between the EAM and the corresponding CT generated attenuation map (LA=left atrium; LIPV = left interior pulmonary vein; LSPV = left superior pulmonary vein; RIPV = right inferior pulmonary vein; RSPV = right superior pulmonary vein).

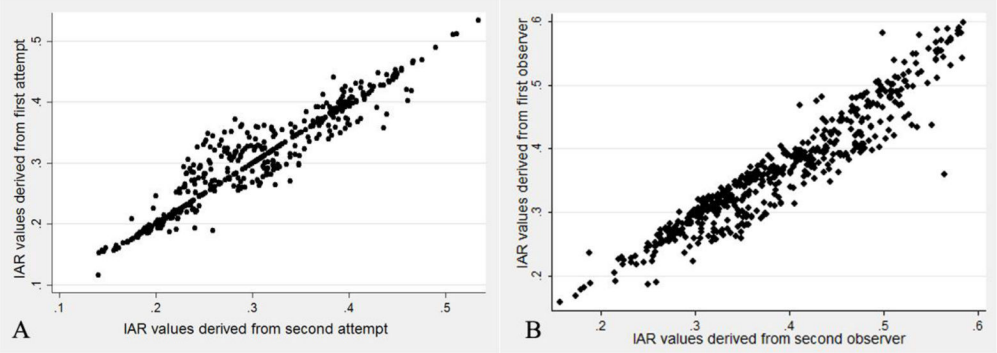

Figure 3. Intra- and Inter-observer Agreement

Panel A: Intra-observer variability – IAR measures derived from repeated contours from the same observer for 5 CT studies. Panel B: Inter-observer variability – IAR measures derived from contours from two different observers for 5 CT studies.

Table 1

Patient characteristics

Patient no.	Age (years)	Male Sex	AF*, Type	Duration of AF years	Hypertension	Diabetes	Vascular	$CHADS_2$ score	BMI† (Kg/m^2)
1	58	NO	Persistent	2.5	YES	NO	NO	1	21.4
2	65	NO	Paroxysmal	31	YES	Impaired	NO	2	31.6
3	40	YES	Paroxysmal	16	YES	NO	NO	1	28.4
4	60	YES	Paroxysmal	6	YES	NO	YES	1	27.8
5	57	YES	Persistent	5	YES	NO	NO	1	28.8
6	77	NO	Paroxysmal	13	YES	YES	YES	3	29.7
7	62	NO	Persistent	7	YES	YES	NO	2	38.8
8	40	YES	Paroxysmal	3	NO	NO	NO	0	27.8
9	65	YES	Paroxysmal	3	YES	NO	NO	1	29.2
10	52	YES	Paroxysmal	7	NO	NO	NO	0	25.5
11	70	NO	Persistent	2	YES	NO	YES	1	38.6
12	60	NO	Paroxysmal	8	YES	NO	NO	1	40.24
13	67	NO	paroxysmal	7	YES	NO	NO	1	23.98
14	64	NO	Persistent	10	NO	NO	NO	3	27.47
15	64	YES	Persistent	3	NO	NO	NO	0	29.18
16	54	YES	Paroxysmal	9	YES	NO	NO	1	27.3
17	62	NO	Persistent	5	NO	NO	NO	0	26.6
18	64	YES	Paroxysmal	5	YES	NO	YES	1	24.6
19	77	NO	Persistent	23	YES	NO	NO	2	33.8
20	58	YES	Paroxysmal	3	NO	NO	NO	0	20.4

*AF = atrial fibrillation,

†BMI = body mass index

Table 2

Liner mixed Model Results

Log bipolar	Coefficients	P value	95% Confidence Interval	
IAR	0.252	0.046	0.005	0.499
Age	0.004	0.725	−0.018	0.026
Male sex	0.213	0.344	−0.228	0.653
BMI	0.007	0.754	−0.389	0.536
LA volume	−0.001	0.934	−.009	0.008

Model clustered by patient and adjusted for the effects of left atrial regions as a level 2 variable. IAR= image attenuation ratio; BMI=body mass index; LA=left atrium